

# Beyond Optimization: Intelligence as Metric-Topology Factorization under Geometric Incompleteness

Xin Li

*Department of Computer Science  
University at Albany  
Albany, NY 12222, USA*

XLI48@ALBANY.EDU

Editor: TBD

## Abstract

Contemporary machine learning systems largely equate intelligence with optimization: the ability to search for solutions within a fixed representational geometry. While effective in static settings, this view struggles under distributional shift, task permutation, and continual learning, where even mild topological transformations can invalidate previously learned solutions and induce catastrophic forgetting. We propose Metric-Topology Factorization (MTF) as a unifying geometric principle underlying intelligence. MTF formalizes intelligence not as navigation through a fixed maze, but as the ability to reshape the metric structure of the representation space so that desired behaviors emerge as stable attractors. In this view, learning corresponds to metric contraction, a controlled deformation of a Riemannian geometry, while task identity and environmental variation are encoded topologically and stored separately in memory.

We show that any fixed metric is inherently geometrically incomplete: for any local metric representation, there exist topological transformations that render it singular or incoherent. This geometric incompleteness implies an unavoidable stability-plasticity tradeoff for weight-based learning systems. MTF resolves this limitation by explicitly factorizing stable topological structure from plastic metric warps, enabling rapid adaptation through active geometric switching rather than re-optimization. Building on this foundation, we introduce the Topological Urysohn Machine (TUM) as a computational architecture that implements MTF through memory-amortized metric inference (MAMI). TUM separates spectral task signatures from amortized metric transformations, allowing a single learned geometry to be reused across permuted, reflected, or parity-altered environments. We demonstrate that this factorization explains robustness to task reordering, resistance to catastrophic forgetting, and the ability to generalize across topological transformations that defeat conventional continual learning methods such as elastic weight consolidation.

**Keywords:** Metric-Topology Factorization (MTF); Geometric Incompleteness; Continual Learning; Stability-Plasticity Tradeoff; Memory-Amortized Metric Inference (MAMI); Topological Urysohn Machine (TUM); Catastrophic Forgetting; Topological Condensation; Metric Contraction/Collapse

## 1 Introduction

Despite remarkable empirical progress, contemporary machine learning systems still struggle with a fundamental limitation: they are brittle under topological change Parisi et al. (2019). Tasks that differ only by permutation, reflection, or parity alternation often re-

quire extensive retraining, frequently inducing catastrophic forgetting of previously learned behavior Kirkpatrick et al. (2017); French (1999). This fragility persists even in highly overparameterized models and exposes a deeper issue that is not resolved by scale alone Allen-Zhu et al. (2019).

At a conceptual level, most learning algorithms, including contemporary deep learning frameworks Goodfellow (2016), implicitly equate intelligence with search. In this paradigm, a model’s architecture defines a fixed representational geometry, and learning is reduced to a high-dimensional navigation problem Russell and Norvig (1995): the traversal of a non-convex loss landscape to locate parameter configurations that minimize empirical risk. Under this view, generalization is framed as the discovery of low-error basins within a static manifold, where the “maze” is defined by the rigid constraints of the data distribution and the inductive biases of the network Geman et al. (1992). While highly effective in stationary environments, this search-centric paradigm is fundamentally brittle Wang et al. (2024). It fails when the underlying manifold undergoes topological or geometric deformation. In such cases, the maze is not merely traversed but fundamentally altered; even mild topological shifts can decouple learned representations from their functional targets, rendering prior knowledge inaccessible and inducing catastrophic interference McCloskey and Cohen (1989).

We argue that this failure mode reflects a deeper representational limitation Bengio et al. (2013). Any fixed metric representation is inherently *geometrically incomplete*: there exist topological transformations under which the metric becomes singular, incoherent, or misaligned with task structure Milnor (1963). This observation motivates reframing intelligence not as the pursuit of a universal metric, but as the capacity to manage the interplay between metric structure and topology Lee (2018). To formalize this idea, we introduce *Metric-Topology Factorization (MTF)*. MTF decomposes representation into two complementary components: a *topological* component that captures task identity and global structure, and a *metric* component that governs local geometry and guides inference. Learning, under this view, corresponds to controlled *metric contraction*, a deformation of the representation geometry that shapes the flow of inference, while memory stores reusable topological indices that enable rapid reconfiguration Amari (1998).

The MTF perspective leads to a fundamental shift in the reconciliation of stability and plasticity Wang et al. (2024). Rather than protecting individual parameters, as in elastic weight consolidation Kirkpatrick et al. (2017) and related approaches, MTF preserves stability by keeping topology invariant while allowing metrics to be actively switched or reoriented Martens (2020). As a result, adaptation to new tasks proceeds through geometric control rather than re-optimization, enabling rapid generalization across permuted or parity-altered environments Masse et al. (2018). Building on MTF, we propose the *Topological Urysohn Machine (TUM)* as a computational architecture that implements this factorization through memory-amortized metric inference (MAMI) Gershman and Goodman (2014). TUM separates spectral task signatures from amortized metric warps, allowing a single learned geometry to be reused across distinct task topologies. This separation explains why TUM-based systems can resist catastrophic forgetting French (1999) and adapt efficiently to topological shifts that defeat conventional weight-based learners. Under MTF, intelligence is not the ability to search a fixed maze, but the ability to reshape the metric so the solution becomes the bottom of a bowl, while topology determines which bowl to use (refer to the Bowl-Maze analogy in Fig. 1).

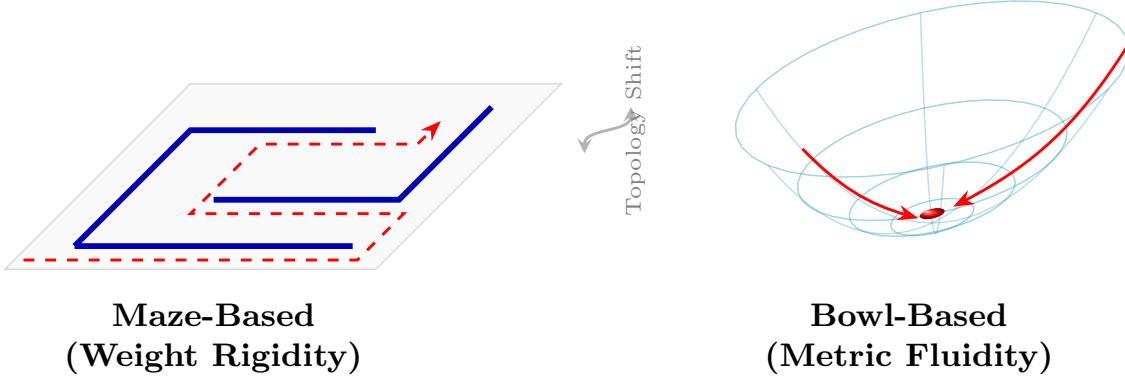


Figure 1: **The Bowl-Maze Analogy: From path-finding to metric contraction.**

*Left: The Maze (Topological Obstruction).* Conventional learning systems, such as stochastic gradient descent (SGD) and elastic weight consolidation (EWC), treat intelligence as navigation within a fixed, complex geometry. In this “Maze”-based regime, topological features, such as holes, walls, or parity flips, manifest as local minima and dead-ends. Learning is a slow, procedural search for a valid path, which is easily invalidated by any change in the environment’s topology.

*Right: The Bowl (MTF).* Under the MTF framework, intelligence is redefined as the ability to shape the metric structure of the space. Instead of searching for paths, the agent performs *topological indexing* to switch into a coordinate system where the solution emerges as a stable, global attractor. By warping the maze into a “Bowl” (topological condensation followed by metric contraction), the agent replaces complex navigation with a simple downhill descent, ensuring that once the topology is identified, the solution is both reachable and consistent.

**Contributions.** This paper makes four primary contributions.

- We identify *geometric incompleteness* as a fundamental limitation of fixed-metric learning systems, thereby formalizing why stability and plasticity cannot be achieved simultaneously with static parameterizations.
- We introduce *Metric-Topology Factorization (MTF)* as a principled resolution to the stability-plasticity dilemma, separating stable topological structure from plastic metric control. MTF is the geometric implementation of Structure-before-Specificity (spatial cognition) and Search-before-Stabilization (temporal control) principles.
- We propose the *Topological Urysohn Machine (TUM)* as a computational architecture that implements MTF through memory-amortized metric inference, enabling rapid adaptation to topological transformations without catastrophic forgetting.
- We formulate *Memory-Amortized Metric Inference (MAMI)* as a mechanism for the *Riemannian Unit (RU)* to perform instant metric recall; by indexing learned local geometries via spectral signatures, the system effectively bypasses iterative re-

optimization, transforming continual learning from a weight-correction problem into a dynamic geometric-control task.

## 2 Theoretical Foundation of Geometric Incompleteness

To define energy dissipation and flow, we require a differentiable structure equipped with a notion of angle and length.

**Definition 1 (Riemannian Manifold)** *A Riemannian manifold is a pair  $(\mathcal{M}, g)$ , where  $\mathcal{M}$  is a smooth manifold and  $g$  is a Riemannian metric tensor. For every point  $p \in \mathcal{M}$ ,  $g_p$  defines an inner product  $\langle \cdot, \cdot \rangle_p$  on the tangent space  $T_p\mathcal{M}$ .*

**Definition 2 (The Gradient Operator)** *Given a smooth scalar potential  $E : \mathcal{M} \rightarrow \mathbb{R}$ , the gradient  $\nabla_g E$  is the unique vector field satisfying:  $g(\nabla_g E(p), v) = dE_p(v) \quad \forall v \in T_p\mathcal{M}$ .*

This definition is crucial: it translates the logical desire to minimize  $E$  (a differential 1-form) into a physical movement (a tangent vector). In Euclidean space, the gradient is simply the vector of partial derivatives; on a curved manifold, the metric  $g$  warps this vector, determining the steepest descent path compatible with the geometry Battiti (1992).

**Urysohn’s Lemma and Urysohn-Brouwer Separation** The core logic of the machine relies on the ability to distinguish concepts topologically. We ground this in two related foundational results: one analytical and the other geometric.

**Lemma 3 (Urysohn’s Lemma Urysohn (1925)- The Functional Form)** *Let  $X$  be a normal space and  $A, B$  be disjoint closed subsets of  $X$  (representing distinct logical concepts, e.g.,  $A = \text{“Cat”}$ ,  $B = \text{“Dog”}$ ). There exists a continuous function  $f : X \rightarrow [0, 1]$  such that:  $f(A) = \{0\}$ ,  $f(B) = \{1\}$ . In metric spaces, this function can be constructed explicitly using distance functions (e.g.,  $f(x) = \frac{d(x, A)}{d(x, A) + d(x, B)}$ ), serving as the continuous logic gate of our topological Urysohn machine.*

While Urysohn’s Lemma gives us a gradient, the **Urysohn-Brouwer Lemma** (often central to dimension theory Hurewicz and Wallman (2015)) gives us the geometry of the decision boundary.

**Lemma 4 (Urysohn-Brouwer Lemma Willard (2012) - The Geometric Form)** *Let  $X$  be a normal space and  $A, B$  be disjoint closed sets. Then there exists a closed set  $C$  (a separator) such that  $X \setminus C = U \cup V$ , where  $U$  and  $V$  are disjoint open sets containing  $A$  and  $B$  respectively.*

A central assumption in many learning systems is that a sufficiently expressive metric representation can, in principle, accommodate all relevant task variations Bengio et al. (2013). Under this view, failure on a new task is attributed to insufficient optimization, capacity, or data Kaplan et al. (2020). Inspired by Urysohn’s lemma, we show that this assumption is false in a precise geometric sense. We argue that any attempt to impose a globally funnel-shaped descent landscape over a semantically complex state space encounters a fundamental topological obstruction Esmaeili et al. (2023). The topological obstruction

is not algorithmic, but structural Esmaeili et al. (2023): it arises from the incompatibility between global metric contraction and nontrivial topology Lee (2018).

We formalize the topological obstruction using tools from Morse theory Milnor (1963), which link the critical structure of smooth functions to the topology of the underlying manifold. Consider a learning system whose inference dynamics are governed by gradient descent Ruder (2016) on a smooth energy (or loss) function  $E : \mathcal{M} \rightarrow \mathbb{R}$  defined over a representation manifold  $\mathcal{M}$ . A common design objective is to shape  $E$  so that trajectories globally converge toward a desired solution via a single basin of attraction Khalil (2002). However, this objective implicitly assumes that  $\mathcal{M}$  admits a globally contracting metric structure Hirsch et al. (2012). As we show below, this assumption fails whenever the semantic complexity of the task induces nontrivial topology.

**Definition 5 (Semantic Complexity)** *Let  $\mathcal{M}$  be a smooth, connected, compact manifold of dimension  $d$ . We call  $\mathcal{M}$  **semantically complex** if it has non-trivial intermediate homology:  $\beta_k(\mathcal{M}) := \text{rank } H_k(\mathcal{M}; \mathbb{R}) > 0$  for some  $1 \leq k \leq d - 1$ . Intuitively, semantic complexity indicates the presence of holes, loops, or obstacles that prevent global contraction, such as those found in a torus or Möbius band rather than a sphere.*

Urysohn’s Lemma guarantees that topological distinctions can always be separated by continuous scalar functions. However, such guarantees are purely topological and do not extend to smooth, globally contracting energy landscapes Lee (2018). Once smoothness and gradient dynamics are required, Morse theory imposes strict constraints linking topology to unavoidable saddle structure. The following geometric incompleteness theorem (a continuous counterpart of Gödel’s incompleteness theorem in logic Gödel (1962)) can be viewed as the dynamical counterpart to Urysohn’s Lemma: while topology admits separation, it generically obstructs global metric contraction.

## 2.1 The Geometric Incompleteness Theorem

The necessity of a hybrid topological-metric architecture is not merely an engineering heuristic; it reflects a fundamental topological obstruction to globally funnel-shaped descent on semantically complex state spaces. We formalize this obstruction using Morse theory Milnor (1963), which relates the geometry of an energy landscape (via critical points) to the topology of the underlying manifold (via homology) Hatcher (2002).

**Lemma 6 (No-Saddle Funnel Force Simplicity)** *Let  $E : \mathcal{M} \rightarrow \mathbb{R}$  be a Morse function representing the agent’s energy landscape. If  $E$  possesses no critical points of intermediate index (i.e., no saddles, so  $c_k(E) = 0$  for all  $1 \leq k \leq d - 1$ ), then the topology of  $\mathcal{M}$  is severely constrained. The Morse inequalities imply that all intermediate homology groups vanish:  $H_k(\mathcal{M}) = 0$  for all  $1 \leq k \leq d - 1$ . In the stronger case where  $E$  has a single minimum and no other critical points and assuming  $\nabla E$  is transverse to the boundary  $\partial\mathcal{M}$  so that a standard handle decomposition applies, the manifold  $\mathcal{M}$  must be contractible.*

Lemma 6 gives a one-way implication: if an energy landscape is globally funnel-shaped in the strong Morse sense, i.e., it contains no intermediate-index critical points, then the underlying state manifold cannot support nontrivial intermediate homology Hatcher (2002).

We now take the contrapositive viewpoint. If the semantic state space  $\mathcal{M}$  is *semantically complex* (i.e., it has some  $H_k(\mathcal{M}) \neq 0$  for  $1 \leq k \leq d-1$ ), then a no-saddle funnel is topologically impossible: any structurally stable (Morse) landscape must introduce at least one intermediate-index critical point Milnor (1963). Moreover, since Morse functions are  $C^2$ -dense, this obstruction is generic: even if a designer writes down a smooth  $E$  that appears saddle-free, an arbitrarily small perturbation yields a Morse function that necessarily contains saddles, which yields the following metric-topological incompleteness result.

**Theorem 7 (Metric-Topological Incompleteness)** *Let  $\mathcal{M}$  be a semantically complex manifold. Then the following statements hold:* 1) **Morse Necessity.** Any Morse function  $E : \mathcal{M} \rightarrow \mathbb{R}$  must possess at least one critical point of intermediate index  $k$  with  $1 \leq k \leq d-1$ . Under gradient flow  $\dot{z} = -\nabla_g E$ , such points correspond to saddle-type equilibria; 2) **No-Saddle Obstruction.** There exists no Morse (equivalently, structurally stable) smooth Lyapunov function on  $\mathcal{M}$  whose critical set consists only of minima and maxima; 3) **Genericity.** For any smooth function  $E$ , an arbitrarily small  $C^2$  perturbation  $\tilde{E}$  is Morse and therefore must contain at least one such saddle point.

**Interpretation: The Algorithmic Cost of Topology.** Theorem 7 identifies an unavoidable structural cost imposed by topology. Although stable manifolds of saddle points are measure-zero in idealized continuous gradient flows, they become significant in realistic learning systems. Under discretization (finite step size) or stochastic perturbations (noise), trajectories near saddles exhibit critical slowing down and heightened sensitivity to initialization Freidlin and Wentzell (2012). These unstable separatrices partition the state space into distinct basins of attraction. On a semantically complex manifold, such saddle-induced structure is generically unavoidable. As a consequence, any purely funnel-based optimization scheme that ignores topological separatrices can incur substantial algorithmic costs: long transient dynamics near saddle regions, unstable basin switching, and sensitivity to noise and discretization. In summary, saddles contribute nontrivial chain-recurrent structure Hirsch (1976); Guillemin and Pollack (1974), which is negligible only in the idealized limit of exact continuous-time dynamics.

## 2.2 Worked Example: Parity as a Möbius Twist

We now give a concrete example illustrating how a parity transformation induces nontrivial topology, and why Theorem 7 implies that any globally funnel-shaped (no-saddle) descent scheme must fail generically. The example also clarifies the architectural motivation for a topological navigation phase followed by a metric-collapse phase in the next section.

**Setup: a latent state with parity ambiguity.** Let the latent state be  $(u, s)$  where  $u \in [0, 1]$  is a continuous coordinate (e.g., position along a corridor) and  $s \in \{+1, -1\}$  is a parity bit (e.g., orientation, handedness, or a left-right swap in sensor ordering). Consider the quotient identification  $(0, +1) \sim (1, -1)$ ,  $(0, -1) \sim (1, +1)$ , which glues the two ends with a parity flip. The resulting state space is the *Möbius band*:  $\mathcal{M} \cong ([0, 1] \times \{+1, -1\}) / \sim$ . Intuitively, traversing the  $u$ -direction once flips parity, and two traversals return to the original parity. This is the simplest model of *parity alternation* as a global topological twist rather than a local perturbation Willard (2012).

**Objective: a “single-goal” energy.** The Möbius band is not contractible and has nontrivial topology (it deformation-retracts to a circle), hence it contains a nontrivial 1-cycle. In particular, it has nonzero first Betti number,  $\beta_1(\mathcal{M}) > 0$ , so  $\mathcal{M}$  is semantically complex in the sense of Definition 5 and therefore Theorem 7 applies. Suppose the task is to reach a target semantic state corresponding to some location  $u^*$  *independent of parity* (the goal is the same physical place even if the agent’s sensors are parity-flipped). Formally, the semantic goal set is the parity-invariant subset  $G = \{(u^*, +1), (u^*, -1)\}/\sim \subset \mathcal{M}$ . We would like to construct a smooth Lyapunov energy  $E : \mathcal{M} \rightarrow \mathbb{R}$  whose gradient flow globally funnels all trajectories into  $G$  without requiring “search”. In the Bowl-Maze analogy, this corresponds to shaping a single global bowl whose bottom represents the goal.

**Obstruction: why a global no-saddle funnel cannot exist.** Assume for contradiction that there exists a *Morse* energy  $E$  with a globally funnel-shaped structure: one (or two parity-equivalent) minima at  $G$  and no saddles (no intermediate-index critical points). By Lemma 6, such a no-saddle Morse function would force  $\mathcal{M}$  to have trivial intermediate homology (and in the strongest case, to be contractible). But  $\mathcal{M}$  is a Möbius band and therefore semantically complex, which contradicts Theorem 7(1–2). *Conclusion:* on a parity-twisted state space, any structurally stable smooth energy landscape must introduce at least one saddle-type critical point. Equivalently, any attempt to build a single global “bowl” must contain a separatrix that partitions basins, creating an unavoidable topological navigation burden Hirsch et al. (2012).

**Interpretation: a minimal Morse picture.** Theorem 7 does not merely assert existence but predicts what failure modes must appear. On the Möbius band, the simplest Morse decomposition compatible with  $\beta_1(\mathcal{M}) > 0$  includes: at least one minimum (goal basin) and at least one index-1 critical point (saddle) to account for the nontrivial 1-cycle. Geometrically, the index-1 saddle generates a separatrix that “cuts” the band, turning the global loop into a handle in the Morse handle decomposition. Algorithmically, this saddle region becomes a bottleneck under discretization or noise (critical slowing down and basin sensitivity), consistent with the interpretation in Section 2.1.

**Debugging: Why weight-based learning restarts under parity flips.** A parity flip corresponds to the deck transformation induced by traversing the Möbius cycle once. A learner that encodes task structure only in a fixed local metric (weights) effectively commits to one local trivialization of the bundle. Under a parity flip, that trivialization becomes globally inconsistent: distances and decision boundaries that were coherent in one chart become misaligned in the flipped chart. Because the obstruction is topological, retraining is not merely slow - it is *structurally unavoidable* if the learner lacks a mechanism to represent the parity twist explicitly.

**TUM-RU resolution: topological navigation followed by metric collapse.** The worked example motivates the hybrid architecture implied by Theorem 7. A TUM module performs a discrete *topological identification* step: it detects whether the current trajectory lies on the  $s = +1$  or  $s = -1$  branch (equivalently, which side of the separatrix induced by the saddle), thereby selecting the correct basin. Once the basin is selected, a Riemannian Unit (RU) module performs *metric collapse* within that basin, yielding fast convergence to  $G$  Shazeer et al. (2017). This way, parity alternation is handled by *active geometric*

*switching* (reselecting the chart/metric warp) rather than re-optimizing from scratch Wang et al. (2024). Note that parity alternation can be realized as a Möbius-type topological twist of the semantic state space. On such semantically complex manifolds, Theorem 7 implies that globally funnel-shaped descent without saddles is impossible in the structurally stable (Morse) regime. Therefore, robust intelligence requires a factorized mechanism that negotiates separatrices (topological phase) and then accelerates convergence (metric phase), precisely motivating the TUM-RU hybrid design under the MTF framework. In summary, geometric incompleteness implies that no single metric descent mechanism can simultaneously provide global robustness and local efficiency on semantically complex spaces. The resolution is not to eliminate saddles, but to manage them via MTF - a principled response explicitly separating *topological navigation* from *metric optimization*.

### 3 Intelligence as Metric-Topology Factorization

Section 2 established that on semantically complex manifolds, no single smooth metric descent mechanism can provide globally funnel-shaped dynamics without encountering saddle-induced separatrices. This topological obstruction implies that intelligence cannot be realized as optimization within a fixed representational geometry, which motivates a hybrid architectural design (Fig. 2). A *topological navigation phase* (implemented by the Topological Urysohn Machine, TUM) first negotiates separatrices to identify the correct basin. Once within that basin, a *metric-collapse phase* (implemented by metric contraction or MTF-warp) rapidly accelerates convergence through local geometric contraction.

#### 3.1 Representation Learning via Metric-Topology Factorization

We now introduce *Metric-Topology Factorization (MTF)* as a principled response. MTF resolves geometric incompleteness by explicitly separating the representation of global topological structure from the control of local metric geometry Khalil (2002). The metric-topology separation allows a system to negotiate topological obstructions discretely, while retaining fast metric convergence within topologically coherent regions.

**Definition 8 (Topological Representation)** *Let  $\mathcal{M}$  be a semantic state manifold. A topological representation is a discrete or low-complexity variable  $\tau \in \mathcal{T}$  that indexes the global topological configuration of the state, such as task identity, parity class, or homology class. The map  $\pi : \mathcal{M} \rightarrow \mathcal{T}$  assigns each state to its topological class.*

**Definition 9 (Metric Representation)** *Given a fixed topological class  $\tau \in \mathcal{T}$ , a metric representation is a Riemannian metric  $g_\tau \in \mathcal{G}(\mathcal{M}_\tau)$  defined on the corresponding fiber  $\mathcal{M}_\tau := \pi^{-1}(\tau)$ , which induces local geometric structure and supports efficient gradient-based inference.*

The defining property of MTF is that topological reconfiguration and metric inference commute: once the correct topological class is selected, metric descent proceeds independently of how that class was reached.

**Definition 10 (Metric-Topology Factorization)** *A learning system is said to implement Metric-Topology Factorization (MTF) if its inference dynamics decompose into two*

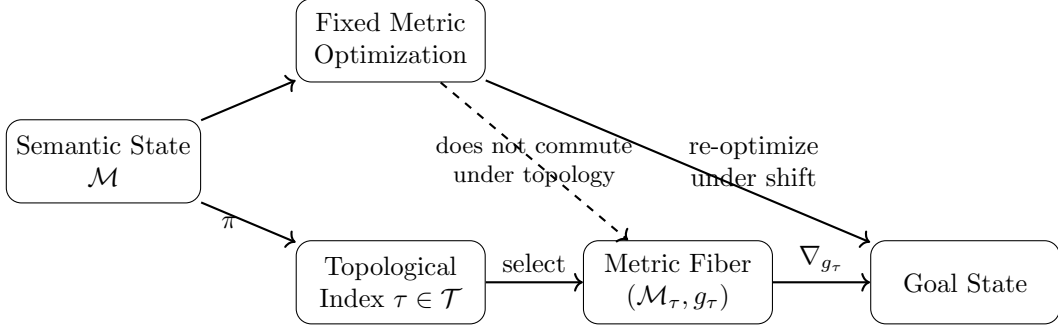


Figure 2: **Metric-Topology Factorization.** *Top:* Unfactorized inference attempts to solve all tasks via optimization in a fixed metric space, requiring re-optimization under topological change. *Bottom:* MTF separates topological identification from metric inference. Once the correct topology is selected, metric descent proceeds within a specialized fiber and is invariant to global topological transformations.

stages: 1) **Topological selection:** infer a topological index  $\tau \in \mathcal{T}$  using coarse, non-metric cues; 2) **Metric inference:** perform gradient-based inference on  $(\mathcal{M}_\tau, g_\tau)$  using a metric specialized to that topology. Equivalently, MTF realizes inference as a composition  $\mathcal{M} \xrightarrow{\pi} \mathcal{T} \xrightarrow{\text{select}} \mathcal{G}(\mathcal{M}) \xrightarrow{\nabla_{g_\tau}} \mathcal{M}_\tau$ .

MTF resolves the obstruction identified in Theorem 7 by construction. Topological complexity is handled discretely through index selection, while metric descent is confined to fibers on which global contraction is possible. Importantly, saddles are no longer algorithmic pathologies to be eliminated. They mark transitions between topological fibers and are handled by the topological phase of inference Hatcher (2002). Within each fiber, the metric phase can safely implement aggressive contraction, recovering the efficiency of funnel-shaped descent without violating topological constraints. MTF also naturally induces a two-component architecture McClelland et al. (1995). A *Topological Urysohn Machine (TUM)* implements the map  $\pi$  and topological selection, while a *Riemannian Unit (RU)* implements metric inference on each fiber. Their interaction realizes memory-amortized inference by reusing metric structure across topologies Gershman and Goodman (2014). In the next subsection, we formalize this architecture and show how the TUM-RU interaction yields rapid adaptation under permutation, parity alternation, and continual learning.

### 3.2 Information Distillation: Topological Condensation vs. Metric Contraction

In the context of the TUM, we define the two-stage process of information distillation (topological condensation vs. metric contraction) as follows Chung (1997):

**Definition 11 (Topological Condensation)** Let  $\mathcal{M} \subset \mathbb{R}^d$  be a data manifold associated with task  $\mathcal{T}$ . Let  $L$  denote the normalized graph Laplacian of the observed point cloud on  $\mathcal{M}$ . **Topological condensation** is the operator  $\Psi_{top}$  that maps the manifold to a discrete

spectral signature  $\Sigma$ :

$$\Psi_{top} : \mathcal{M} \rightarrow \Sigma, \quad \Sigma = \{\lambda_1, \lambda_2, \dots, \lambda_k\} \subset \text{spec}(L) \quad (1)$$

where  $\{\lambda_1, \dots, \lambda_k\}$  are the  $k$ -smallest non-zero eigenvalues. This operation distills the global connectivity and homeomorphism class (e.g., genus, orientability) of the environment into a stable identity key, invariant to local metric perturbations.

Topological condensation produces a *task identity* that is stable under local metric variation. Concretely, the spectral signature  $\Sigma = \Psi_{top}(\mathcal{M})$  serves as an *address* into the memory system: it tells the agent *which topological fiber* of experience it is currently in (e.g., which orientability/parity class or connectivity type), without committing to a particular coordinate system within that fiber Steenrod (1951). The operator  $\Psi_{top}$  serves as the implementation of the topological quotient map  $\pi : \mathcal{M} \rightarrow \mathcal{M}/\sim$ , where the equivalence relation  $x \sim y$  is defined by membership in the same homeomorphism class Hatcher (2002). This condensation ensures that the subsequent metric learning occurs on a topologically flattened fiber, free from the saddle-point obstructions predicted by Morse theory Milnor (1963). MTF uses the discrete identity after condensation to *select and protect* representational resources for the corresponding task family. In other words,  $\Sigma$  is not itself a representation to be optimized; it is a *routing key* that determines *where* metric learning is allowed to act Miller et al. (2016). Given  $\Sigma$ , the memory-amortized metric stage Gershman and Goodman (2014) assigns an *active subspace* in feature space and learns a task-appropriate metric warp within that subspace. This is the role of metric contraction: to implement fast, locally contractive inference *conditioned on* the topological identity  $\Sigma$ , while nulling updates in orthogonal directions to prevent cross-task interference Saha et al. (2021); Farajtabar et al. (2020). We formalize this as follows.

**Definition 12 (Metric Contraction with Subspace Allocation)** *For a task identified by signature  $\Sigma$ , the MAMI engine assigns an **active subspace** defined by an orthogonal projector  $P_\Sigma \in \mathbb{R}^{d \times d}$  with rank  $k := \text{rank}(P_\Sigma)$ . Let  $z \in \mathbb{R}^d$  denote features produced by a shared extractor  $\Phi_\theta$ . The **metric contraction** operator is  $M_\Sigma := P_\Sigma \tilde{W}_\Sigma$ , where  $\tilde{W}_\Sigma$  is a (learned) linear whitening warp such that, for  $x \sim \mathcal{T}_\Sigma$ ,*

$$\mathbb{E}[(M_\Sigma z)(M_\Sigma z)^\top] = \mathbb{E}[(P_\Sigma \tilde{W}_\Sigma z)(P_\Sigma \tilde{W}_\Sigma z)^\top] \approx \frac{1}{k} P_\Sigma. \quad (2)$$

*Equivalently, the representation is (approximately) isotropic within  $\text{Range}(P_\Sigma)$  and carries no energy in the orthogonal complement.*

**Remark 13 (Relation to Iterative Normalization)** *The operator  $\tilde{W}_\Sigma$  can be viewed as an amortized, task-conditioned extension of iterative normalization Huang et al. (2019). While standard iterative whitening (e.g., via Newton-Schulz iterations Higham (2008)) is typically used to improve optimization stability by decorrelating features across a single domain, metric contraction utilizes this mechanism to perform topological quotienting. By enforcing subspace-specific isotropy, the engine ensures that each task-fiber is mapped to an identical Euclidean ‘‘Bowl’’, thereby resolving the geometric incompleteness of the shared backbone.*

**The Metric-Topology Factorization (MTF)** The total inference function  $\mathcal{F}$  of the TUM is defined by the factorization of these condensed components:

$$\mathcal{F}(x) = \mathcal{G}(W_{\Psi_{\text{top}}(x)} \cdot \Phi_{\theta}(x)) \quad (3)$$

where  $\Phi_{\theta}$  is the shared plastic backbone and  $W_{\Sigma}$  is the stable metric warp retrieved from the memory bank using the topological signature  $\Sigma$  as the primary key.

**Theorem 14 (Orthogonal Stability under Subspace-Routed Condensation)** *Let  $\Phi_{\theta} : \mathcal{X} \rightarrow \mathbb{R}^d$  be a shared feature extractor. For distinct signatures  $\Sigma_A \neq \Sigma_B$ , let the MAMI system enforce:* 1) **(Orthogonal routing)** *The assigned projectors are disjoint:  $P_A P_B = 0$ .* 2) **(Subspace-supported warp)** *The whitening warp for task A acts only within its active subspace:*

$$P_A \tilde{W}_A = P_A \tilde{W}_A P_A. \quad (4)$$

3) **(Routed updates)** *The parameter update  $\Delta\theta_B$  for task B is constrained such that for all  $x \in \text{supp}(\mathcal{T}_A)$ , the induced feature perturbation  $\Delta z(x) = \Phi_{\theta+\Delta\theta_B}(x) - \Phi_{\theta}(x)$  satisfies  $P_A \Delta z(x) = 0$ . Define the condensed representation for task A as  $\hat{z}_A(x) = P_A \tilde{W}_A \Phi_{\theta}(x)$ . Then  $\hat{z}_A$  is first-order invariant under learning task B:  $\hat{z}'_A(x) = \hat{z}_A(x)$  for all  $x \in \text{supp}(\mathcal{T}_A)$ , and consequently the change in the task-A loss satisfies  $\mathcal{L}_A(\theta + \Delta\theta_B) = \mathcal{L}_A(\theta) + o(\|\Delta\theta_B\|)$ .*

## 4 Algorithmic Implementations of TUM and MAMI

MTF separates inference into a *topological* phase and a *metric* phase. The role of the TUM is to implement the former: to infer and index the global topological configuration of the current state before metric-based inference is applied later.

### 4.1 Parity Handling as Topological Switching

The Möbius/parity example in Sec. 2.2 illustrates the core operational role of the TUM. Conceptually, the TUM does not “optimize a trajectory” in a fixed geometry. Instead, it identifies *which representation space* (i.e., which topological fiber and associated metric) the current trajectory should inhabit Hirsch et al. (2012). This distinction is essential on semantically complex manifolds: by Theorem 7, saddle-induced separatrices are generically unavoidable, so a single globally funnel-shaped metric cannot eliminate basin boundaries. The correct response is therefore not to “push harder” with optimization, but to *switch* to the appropriate geometric regime once the global topology is recognized.

**Definition 15 (Spectral Signature and Topological Memory)** *Let  $\mathcal{M}$  be a semantic state manifold equipped with an observation map  $\phi : \mathcal{M} \rightarrow \mathbb{R}^n$ . A spectral signature is a low-dimensional, discrete, or quantized representation  $\sigma = \mathcal{S}(\phi(x)) \in \Sigma$  that is invariant to local metric deformations yet sensitive to global topological structure, such as parity, permutation class, or homology class. Let  $\mathcal{G}(\mathcal{M})$  denote the space of admissible Riemannian metrics on  $\mathcal{M}$ . A topological memory is a key-value map  $\mathcal{M}_{\text{mem}} : \Sigma \rightarrow \mathcal{G}(\mathcal{M})$ , which associates each signature  $\sigma$  with a task-appropriate metric warp  $g_{\sigma}$  (or, equivalently, a metric-condensation operator defined on the corresponding fiber).*

Definition 15 makes precise the separation enforced by MTF: the signature  $\sigma$  is an *identity key* (topology), while  $g_\sigma$  is an *efficiency mechanism* (metric). In particular,  $\sigma$  is not a continuous representation to be optimized; it is a discrete decision variable that selects which metric geometry should be active.

**Parity as a signature on a Möbius-type space.** In the Möbius toy world of Section 2.2, the topological ambiguity is parity: a traversal of the nontrivial cycle flips the agent’s orientation. Accordingly, the TUM computes a parity-sensitive signature  $\sigma \in \{+, -\}$ , which identifies the current “sheet” of the Möbius band. Crucially,  $\sigma$  is stable under local metric deformation along the continuous coordinate  $u$ , but flips under the global topological twist. Therefore, parity alternation is expressed as a change in *topological identity* rather than as a new task.

**Memory indexing and metric reuse.** The topological memory stores a small set of metric warps keyed by  $\sigma$  Miller et al. (2016):  $\mathcal{M}_{\text{mem}}(+) = g_+$ ,  $\mathcal{M}_{\text{mem}}(-) = g_-$ . These warps are related by a coordinate reflection (they implement the same semantic objective under opposite orientations), but they are *distinct* as metric geometries because they correspond to different global identifications of the state space. Once  $\sigma$  is identified, inference proceeds by applying the retrieved metric warp within the appropriate fiber, turning what would otherwise be a global search problem into a locally contractive descent.

**Definition 16 (Active Geometric Switching)** Active geometric switching *is the discrete operation  $g_\sigma \mapsto g_{\sigma'}$  with  $\sigma' \neq \sigma$ , triggered by a change in spectral signature, while preserving the underlying semantic objective.*

Active switching is the operational counterpart of the Bowl-Maze analogy (Fig. 1): a parity flip does not require re-learning the “bowl”; it requires flipping to the correct bowl. In practice, switching occurs at the level of *which metric is applied* (or which subspace is activated), rather than at the level of rewriting shared parameters.

**Why this prevents catastrophic forgetting.** Conventional continual-learning methods implicitly bind task identity into metric parameters Wang et al. (2024). Under topological change, the learner attempts to force incompatible global structures into a single metric, creating destructive interference. By contrast, the TUM enforces a clean separation:

1. topological identity is stored discretely via the signature  $\sigma$ ,
2. metric structure is reused conditionally by retrieving  $g_\sigma$ ,
3. topological updates do not overwrite metric structure associated with other signatures.

In this view, “forgetting” is not an inevitable consequence of learning, but a consequence of *misidentifying* topology or conflating topology with metric adaptation.

## 4.2 Memory-Amortized Metric Inference (MAMI)

Once the TUM has identified the appropriate topological class  $\tau \in \mathcal{T}$  via a spectral signature, inference proceeds within the corresponding fiber  $\mathcal{M}_\tau = \pi^{-1}(\tau)$  Steenrod (1951). On this fiber, global topological obstructions have been factored out, and aggressive metric

**Algorithm 1** MAMI: Signature/Search  $\rightarrow$  Route/Retrieve  $\rightarrow$  Condense/Contract

---

**Require:** Stream  $\mathcal{D} = \{(x_t, y_t)\}_{t=1}^T$ , shared feature extractor  $\Phi_\theta$ , readout  $\mathcal{G}$ , topological condenser  $\Psi_{\text{top}}$ , signature-to-memory map  $\mathcal{M}_{\text{mem}}$ , subspace projectors  $\{P_\Sigma\}$ , whitening warps  $\{\tilde{W}_\Sigma\}$ , learning rate  $\alpha$ , condensation update interval  $K$

**Ensure:** Updated parameters  $\theta$  and memory entries  $\{(P_\Sigma, \tilde{W}_\Sigma)\}$

- 1: **for**  $t = 1$  to  $T$  **do**
- 2:   **Topological identification:**  $\Sigma_t \leftarrow \Psi_{\text{top}}(x_t)$  ▷ discrete signature / key
- 3:   **Memory indexing:** retrieve  $(P_{\Sigma_t}, \tilde{W}_{\Sigma_t}) \leftarrow \mathcal{M}_{\text{mem}}(\Sigma_t)$
- 4:   **metric contraction/collapse (encode):**  $z_t \leftarrow \Phi_\theta(x_t)$ ;  $\hat{z}_t \leftarrow P_{\Sigma_t} \tilde{W}_{\Sigma_t} z_t$
- 5:   **Prediction:**  $\hat{y}_t \leftarrow \mathcal{G}(\hat{z}_t)$ ;  $\ell_t \leftarrow \mathcal{L}(\hat{y}_t, y_t)$
- 6:   **Routed update (write-gated):** compute  $g_t \leftarrow \nabla_\theta \ell_t$  and apply an update that affects only the active subspace for  $\Sigma_t$ :  $\theta \leftarrow \theta - \alpha \Pi_{\Sigma_t}(g_t)$ , where  $\Pi_{\Sigma_t}$  denotes the parameter-gradient routing operator induced by  $P_{\Sigma_t}$  (e.g., via feature-gradient projection or subspace-gated adapters).
- 7:   **if**  $t \bmod K = 0$  **then**
- 8:     **Condensation refinement (memory write):** update  $\tilde{W}_{\Sigma_t}$  to better satisfy the subspace whitening condition  $\mathbb{E}[(P_{\Sigma_t} \tilde{W}_{\Sigma_t} z)(P_{\Sigma_t} \tilde{W}_{\Sigma_t} z)^\top] \approx \frac{1}{k} P_{\Sigma_t}$  using an iterative whitening routine (e.g., Newton–Schulz).
- 9:     Optionally update/allocate  $P_{\Sigma_t}$  if the active rank  $k$  must expand (subject to orthogonality constraints).
- 10:   **end if**
- 11: **end for**
- 12: **return**  $\theta, \{(P_\Sigma, \tilde{W}_\Sigma)\}$

---

contraction becomes feasible. We refer to this second stage as *memory-amortized metric inference* (MAMI), as illustrated by Algorithm 1. Its role is not to identify the task, but to efficiently solve it once the correct topological context has been selected.

**Metric collapse on a fixed fiber.** Once the topological signature has been identified and the corresponding memory entry retrieved, the metric phase of MAMI operates on the selected fiber  $\mathcal{M}_\tau = \pi^{-1}(\tau)$  by *routing* representation and updates through a task-specific geometry. Concretely, the memory returns an active-subspace projector  $P_\tau$  together with a learned metric-condensation warp  $\tilde{W}_\tau$ , inducing the effective metric operator  $M_\tau := P_\tau \tilde{W}_\tau$ ,  $\hat{z} = M_\tau \Phi_\theta(x)$ . Inference and learning are performed using the condensed representation  $\hat{z}$ , with gradients *write-gated* so that parameter updates affect only the active subspace associated with  $\tau$  (Algorithm 1). Equivalently, this implements gradient descent in a task-conditioned Riemannian geometry,  $\dot{z} = -\nabla_{g_\tau} E(z)$ , where  $E$  is a task-dependent energy on  $\mathcal{M}_\tau$  Absil et al. (2008). Because the fiber  $\mathcal{M}_\tau$  is topologically simple relative to the full space  $\mathcal{M}$ , the retrieved geometry can be shaped to be strongly contractive toward the goal Wensing and Slotine (2020). We refer to this geometry-shaping as *metric collapse*: the progressive reduction of effective volume in representation space along task-relevant directions, realized operationally by subspace allocation and iterative condensation (e.g., whitening toward an isotropic/ETF-like structure) within  $\text{Range}(P_\tau)$ . A failed (topologically inconsistent) collapse will generate hallucination instead of abstraction.

**Amortization through memory.** Crucially, the metric  $g_\tau$  is not learned from scratch for each episode. Instead, it is *stored* and *progressively refined* across experiences that share the same topological signature  $\tau$ . This reuse constitutes amortization, but in a sense that is structurally different from classical *amortized inference* in probabilistic reasoning Gershman and Goodman (2014). In the Gershman-Goodman formulation, amortization typically refers to learning a direct mapping (e.g., a recognition model) that approximates posterior inference across a distribution of queries, thereby replacing per-query iterative inference with a feedforward computation. Here, by contrast, what is amortized is not a posterior *mapping* but a *geometry*: the system amortizes inference by caching and updating a task-conditioned *Riemannian metric* that reshapes the local landscape so that subsequent inference becomes rapidly contractive. Operationally, our amortization is realized as a memory-indexed retrieve-and-refine loop: search/signature  $\rightarrow$  retrieve/route  $\rightarrow$  contract/condense. The signature stage identifies the relevant topological fiber; the retrieve/route stage selects the corresponding metric warp from memory; and the contract/condense stage performs fast metric collapse within that fiber. Importantly, refinement updates the stored geometry  $g_\tau$  (or its parameterization, e.g., a whitening warp) using accumulated experience, without overwriting metrics associated with other signatures McCloskey and Cohen (1989). As experience accumulates, the retrieved metric increasingly approximates an optimal local geometry for the entire topological class, so that inference cost decreases with reuse, not because the system learns a single global recognition mapping, but because it learns *which geometry to activate* and *how to make that geometry maximally contractive* for that class.

**Relation to Equiangular Tight Frame (ETF).** Under repeated metric collapse across diverse but topologically aligned tasks, the induced geometry approaches a maximally uniform configuration. In finite dimensions, this limiting structure corresponds to an *Equiangular Tight Frame (ETF)* Papyan et al. (2020), which minimizes redundancy while preserving separability. From the MTF perspective, ETFs arise not as design choices, but as fixed points Granas et al. (2003) of MAMI under repeated exposure to structurally similar tasks. Because metric inference operates conditionally on a topological index, updates to  $g_\tau$  do not interfere with metrics associated with other indices. Catastrophic forgetting is therefore avoided by construction Kirkpatrick et al. (2017). Forgetting can only occur if the spectral signature is misidentified or the memory association between  $\tau$  and  $g_\tau$  is corrupted. Neither failure mode arises from metric optimization itself.

**Summary.** The TUM implements the topological half of MTF. By computing signatures and using them to index metric memory, the TUM resolves the geometric incompleteness identified in Section 2.1. Parity alternation and Möbius-type twists are handled through active geometric switching rather than re-optimization, transforming topological complexity from an algorithmic burden into a discrete control signal. MAMI completes the metric half of MTF by providing fast, stable convergence within topologically coherent fibers. By separating topological identification from metric contraction, the architecture achieves both robustness and efficiency without violating the geometric constraints. Importantly, this separation preserves conceptual clarity: Urysohn-type mechanisms are confined to topology, while metric inference is treated as a reusable geometric primitive.

## 5 Experimental Methodology: Validating Topological Obstruction

To empirically validate the claim that catastrophic forgetting is a consequence of geometric incompleteness in non-stationary manifolds, we design a synthetic “Möbius Latent World.” This environment introduces a *topological obstruction* that forces a single-metric learner into a saddle-point bottleneck during task alternation.

### 5.1 The Möbius Latent Environment

We define a latent manifold  $\mathcal{M}$  characterized by a position  $u \in [0, 1]$  and a binary parity state  $s \in \{+1, -1\}$ . The manifold is endowed with a Möbius topology via the boundary identification  $(0, s) \sim (1, -s)$ . Observations  $x \in \mathbb{R}^4$  are generated via a parity-dependent feature map  $f(u, s)$ :

$$x = \begin{cases} [u, 1 - u, 0, 0]^\top & \text{if } s = +1 \text{ (Task A)} \\ [0, 0, 1 - u, u]^\top & \text{if } s = -1 \text{ (Task B)} \end{cases} \quad (5)$$

The semantic objective is the regression task  $y = u$ . While the goal is invariant to parity, the metric relationship between the feature dimensions and the target is disjoint, necessitating a shift in the internal coordinate system of the learner.

**Methods and Comparative Framework** We compare the performance of the **TUM** against standard architectural baselines:

1. **Plain SGD:** A unified MLP representing a “single-bowl” global metric approach with no task-awareness Bottou et al. (2018).
2. **Elastic Weight Consolidation (EWC):** A regularization-based continual learning method that utilizes the Fisher Information Matrix to constrain parameter drift Kirkpatrick et al. (2017).
3. **MTF-Learner (Proposed):** A Topological Urysohn Machine that utilizes *Topological Condensation* to identify the signature  $\Sigma \in \{s\}$  and retrieves a task-specific warp  $W_\Sigma$  to perform *Subspace-Routed Condensation*.

**Evaluative Metrics** The efficacy of the factorization is measured through three primary lenses:

1. **Adaptation Latency ( $\tau$ ):** Defined as the number of gradient steps  $t$  required to recover performance after a parity flip:  $\tau = \min\{t \mid \mathcal{L}(\theta_t) < \epsilon\}$ , where  $\epsilon = 10^{-3}$  is the convergence threshold.
2. **Subspace Orthogonality ( $\mathcal{O}$ ):** To validate the routing theorem, we measure the absolute cosine similarity between the learned task-specific warps  $W_A$  and  $W_B$ :  $\mathcal{O} = \frac{|\langle \text{vec}(W_A), \text{vec}(W_B) \rangle|}{\|W_A\|_F \|W_B\|_F}$ . A value of  $\mathcal{O} \approx 0$  indicates successful MTF.
3. **Saddle-Point Proxy:** We monitor the gradient norm  $\|\nabla \mathcal{L}\|$  relative to the loss decay rate. A high gradient norm paired with stationary loss indicates that the learner is trapped at the topological separatrix.

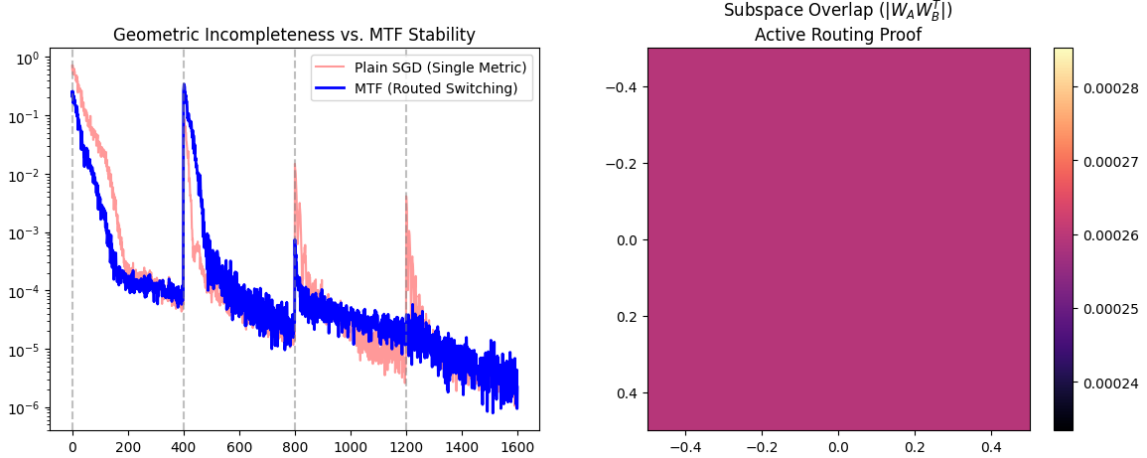


Figure 3: **Empirical Validation of MTF on a Möbius State Space.** (a) The *Plain SGD* learner (red) exhibits characteristic “sawtooth” spikes, indicating a failure to resolve the topological obstruction through a single global metric. The *MTF Learner* (blue) demonstrates near-instantaneous recovery after the initial learning of both parity signatures. (b) Absolute cosine similarity between task-specific metric warps  $W_A$  and  $W_B$  after training with the orthogonality penalty ( $\alpha = 0.5$ ). The vanishing overlap ( $\approx 2.5 \times 10^{-4}$ ) provides empirical proof of the *orthogonal routing* required for representation stability.

**Experimental Schedule and Result** The learner is subjected to a sequence of  $N$  parity alternations. Each task phase consists of  $T = 500$  steps. This schedule tests both the *plasticity* of the model (initial learning of Task B) and its *stability* (zero-shot recall of Task A during the second rotation). Figure 3 provides a minimal empirical test of the central claim of MTF on a parity-twisted (Möbius) state space.

Panel (a) contrasts a *single-metric* learner trained with plain SGD against an *MTF learner* that infers a parity signature and routes inference through a signature-indexed metric warp. Under parity alternation, the SGD baseline exhibits the characteristic “sawtooth” pattern—sharp loss/accuracy degradation immediately after each parity flip, followed by slow re-learning—consistent with the topological obstruction that prevents a single global “bowl” from remaining funnel-shaped across both orientations. In contrast, after the MTF learner has encountered both parities (e.g., after  $t > 800$ ), performance recovers nearly instantaneously at each subsequent flip (note the absence of spike after  $t > 1200$ ), indicating that adaptation is achieved by discrete geometric switching rather than by re-optimization.

Panel (b) verifies the *mechanism* underlying this stability by directly visualizing the interaction between the two parity-specific metric warps. Let  $W_A$  and  $W_B$  denote the learned linear warp operators (rows/filters) associated with the positive- and negative-parity signatures. We plot the absolute matrix product  $|W_A W_B^T| \in \mathbb{R}^{k_A \times k_B}$ , where the *vertical axis* indexes the basis directions of the active subspace used for parity A (i.e., the individual filters/coordinates produced by  $W_A$ ), and the *horizontal axis* indexes the basis directions

of the active subspace used for parity  $B$ . Each pixel  $(i, j)$  measures the magnitude of the dot product  $|\langle (W_A)_{i,:}, (W_B)_{j,:} \rangle|$ , i.e., how strongly the  $i$ -th condensed coordinate of task  $A$  aligns with the  $j$ -th condensed coordinate of task  $B$  in the original feature space. If the two routed subspaces are orthogonal, then every such cross-inner-product vanishes and  $W_A W_B^\top \approx 0$ . Empirically, the heatmap is nearly uniform at (near-)zero intensity, indicating that *all* cross-alignment terms are suppressed simultaneously, which provides direct evidence for the *orthogonal routing* condition ( $P_A P_B = 0$  in Theorem 14). In other words, the uniform near-zero overlap observed in Panel (b) is the empirical signature of the theorem’s mechanism: *subspace-routed condensation creates disjoint active manifolds, which in turn yield first-order invariance and prevent cross-parity interference*.

## 5.2 The Betti-Complexity Paradox: Topological Obstructions to Convergence

To evaluate the relationship between manifold topology and learning stability, we conducted a series of experiments on synthetic datasets with controlled first Betti numbers ( $\beta_1 \in \{0, 1, 2, 4\}$ ). By holding local geometric properties constant and varying only the global connectivity (number of obstacles), we isolate the effect of topological complexity on the loss landscape.

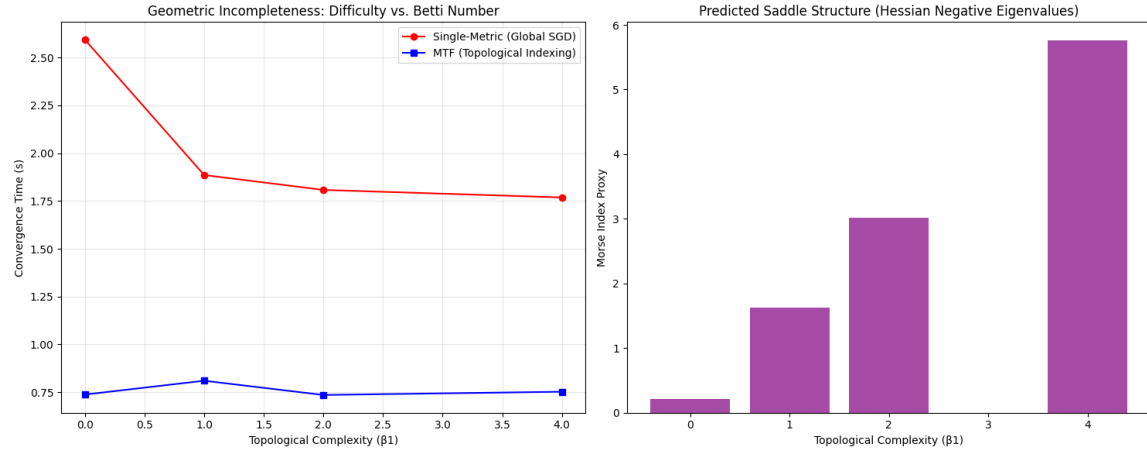


Figure 4: **Impact of Topological Complexity on Learning Stability.** (Left) Convergence time as a function of the first Betti number  $\beta_1$ . The *Single-Metric Learner* (red) exhibits a super-linear increase in training time, while the **MTF Learner** (blue) remains invariant to topological genus. (Right) A proxy for the Morse Index, measured via the density of negative Hessian eigenvalues. Higher topological complexity necessitates a more convoluted loss surface with a higher density of saddle points for unfactorized models.

**Morse-Theoretic Implications** The results in Figure 4 provide empirical weight to our claim that *geometric incompleteness* scales with the genus of the state space. According to Morse theory, the global topology of the manifold constrains the critical points of any

smooth mapping defined over it. As  $\beta_1$  increases, the Single-Metric Learner is forced to accommodate additional “holes” within a single global coordinate chart, leading to the emergence of high-index saddle points (Figure 4, Right). These saddles act as dynamical bottlenecks, trapping gradient descent in regions of high gradient norm but low progress. Conversely, the **MTF approach** utilizes the *spectral signature* of the graph Laplacian to perform a topological switch. By indexing disjoint representation fibers, MTF effectively “unwraps” the manifold, reducing the required Morse complexity of each individual fiber and allowing for consistent convergence times regardless of the global Betti number.

### 5.3 Case Study of Continual Learning: Sequential Permuted MNIST

To evaluate the comparative performance of the **Memory-Amortized Metric Inference (MAMI-MTF)** framework against established synaptic consolidation baseline such as Elastic Weight Consolidation (EWC) Kirkpatrick et al. (2017), we conduct a large-scale sequential learning experiment on the Permuted MNIST benchmark. Unlike standard MNIST, each task in this sequence consists of a unique, fixed random permutation of the image pixels, creating a set of tasks with identical semantic targets but disparate topological input distributions.

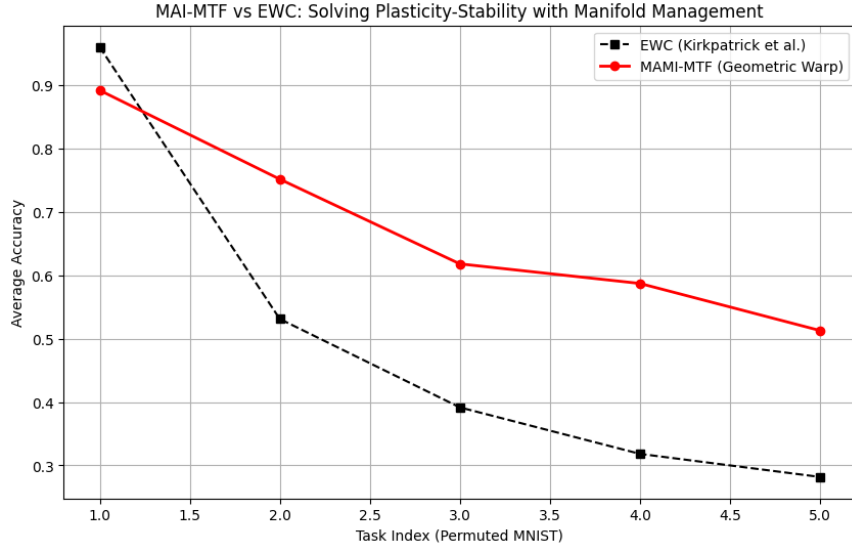


Figure 5: **Continual Learning Performance on Permuted MNIST.** Comparison of *Average Accuracy* over a sequence of 5 permuted tasks. While *Elastic Weight Consolidation (EWC)* (black) maintains higher stability than naive fine-tuning, it exhibits a characteristic “stiffness” as the Fisher constraints accumulate, leading to a performance plateau. The **MAMI-MTF** approach (red) achieves superior plasticity by treating the network as a fluid coordinate system, utilizing iterative Newton-Schulz whitening to amortize the metric warp across task boundaries.

**Performance Analysis and Weight Stiffness** The results in Figure 5 highlight a fundamental advantage of the MTF. In the **EWC** baseline, the model attempts to find a set

of weights  $\theta^*$  that lie in the intersection of low-error regions for all previous tasks. As the number of tasks increases, this intersection shrinks, increasing the “stiffness” of the network and hindering the learning of new task signatures. Conversely, **MAMI-MTF** avoids weight-locking. Instead of preserving static weights, it preserves the *manifold geometry* through an active memory switch. By recalling a task-specific *metric projection*, the model can repurpose the same physical neurons to represent distinct concepts without interference. This allows the system to maintain a high learning velocity even in the late stages of the task sequence, effectively resolving the stability-plasticity dilemma Wang et al. (2024).

## 6 Discussion and Implications

This work proposes a shift in how intelligence is formally characterized. Rather than viewing intelligence as the ability to optimize within a fixed representational space, we argue that intelligence is the capacity to *manage representation itself* under conditions of geometric incompleteness. MTF provides a structural resolution to this problem by separating global topological organization from local metric inference.

### 6.1 Geometric Resolution of the Bias-Variance Dilemma

A central challenge in machine learning theory is the *bias-variance dilemma* Geman et al. (1992), which posits an unavoidable tradeoff between a model’s ability to minimize empirical risk (plasticity) and its sensitivity to stochastic fluctuations (stability). Conventional learning frameworks, operating within a fixed-metric paradigm, couple these quantities: increasing the degrees of freedom to reduce bias inherently increases the variance across task boundaries, manifesting as catastrophic interference. MTF overcomes this dilemma by decoupling these quantities into orthogonal geometric channels. We formalize this resolution through the following mechanisms:

1. **Geometric Orthogonality:** The TUM functions as a *topological variance buffer* by separating task identity from local geometry. In the parity/Möbius setting, a parity flip changes the global identification of the state space (orientation) without changing the underlying semantic objective. The TUM captures this change as a discrete signature and routes inference to the corresponding basin (fiber), so that each parity is represented in a disjoint, signature-indexed regime. Because this identity is stored topologically (as a switchable index) rather than metrically (as shared curvature), it remains invariant to local metric fluctuations and avoids destructive interference: parity alternation triggers *active geometric switching* rather than re-optimization Shazeer et al. (2017), preserving stability without biasing the metric learner toward any single orientation.
2. **Amortized Porosity:** The metric phase of MAMI addresses bias through *memory-conditioned metric contraction*. Rather than learning a task geometry from scratch, the system *retrieves* a signature-indexed warp (active subspace  $P_\Sigma$  and whitening operator  $\hat{W}_\Sigma$ ) Huang et al. (2019) and *refines* it with additional experience. This turns contraction into a reusable resource: each time a topological class reappears, the retrieved metric rapidly collapses the corresponding fiber, shrinking its effective

representational volume and thereby minimizing its long-term footprint. The “porosity” is therefore not a transient artifact of optimization, but a property *maintained by memory*: consolidated tasks occupy compact, isotropic subspaces, while the orthogonal complement remains available for high-plasticity updates, reducing the chance that new learning leaks variance into previously condensed manifolds Farajtabar et al. (2020).

3. **Spectral Gating:** The system uses a simple *spectral diagnostic* of the current representation to decide when to invoke topological identification versus when to commit to metric contraction. In high-entropy regimes, where the representation remains poorly conditioned and task structure is not yet stable, the model prioritizes topological exploration by refining the spectral signature and delaying aggressive metric collapse. Once the representation exhibits a consistent low-dimensional structure (i.e., the spectral signature stabilizes and the active subspace becomes coherent) Belkin and Niyogi (2003), the model switches to metric exploitation, applying subspace-routed condensation (e.g., whitening within  $\text{Range}(P_\Sigma)$ ) to induce fast, contractive inference.

## 6.2 Resolving the Stability-Plasticity Dilemma through Factorization

The stability-plasticity dilemma constitutes a temporal constraint on learning: an agent must remain plastic enough to integrate new distributional information while remaining stable enough to prevent the catastrophic interference of existing representations McCloskey and Cohen (1989). In standard deep learning, this dilemma is exacerbated by the flat nature of the parameter space, where updates for a novel task  $T_{n+1}$  are non-orthogonal to the manifold occupied by task  $T_n$ . MTF provides a geometric bypass to this constraint by partitioning the learning process into two distinct regimes:

- **Topological Stability via Spectral Signatures and Switching:** The TUM ensures stability by encoding task identity as a discrete *spectral signature*  $\Sigma$  that indexes a topological memory. Under global transformations such as parity alternation (Möbius-type twists), the semantic objective is unchanged but the global identification of the state space differs. The TUM treats such events as *topological switches* Miller et al. (2016): a change in  $\Sigma$  triggers *active geometric switching* (selection of the appropriate fiber/metric entry) rather than overwriting a single global representation. Stability is therefore achieved not by freezing weights (as in EWC Kirkpatrick et al. (2017)), but by keeping task identity *discrete and addressable*, preserving the integrity of previously formed basins under topological change.
- **Metric Plasticity via Memory-Conditioned Condensation:** Plasticity is provided by MAMI within the selected fiber. Given a retrieved entry  $(P_\Sigma, \tilde{W}_\Sigma)$ , the system performs *metric contraction* by projecting features into the active subspace and applying a whitening/contractive warp Huang et al. (2019),  $\hat{z} = P_\Sigma \tilde{W}_\Sigma \Phi_\theta(x)$  (Algorithm 1). This local contraction implements *metric collapse*: it concentrates task-relevant variation into a compact, approximately isotropic subspace while leaving the orthogonal complement available for future learning Papyan et al. (2020). Because the warp is *stored and refined* across recurring signatures, plasticity is amorphous.

tized: new episodes reuse an increasingly well-shaped geometry rather than relearning it from scratch, reducing both optimization time and cross-task interference.

By utilizing MAMI, the system can instantly recall the specific Riemannian warp associated with a previously seen topological signature. This transforms the dilemma into a *switching* problem: rather than choosing between stability and plasticity, the agent manages a library of specialized metrics indexed by a stable topological skeleton. In this regime, the system avoids the Saturation limit typical of regularized systems like EWC Kirkpatrick et al. (2017). While EWC becomes increasingly rigid as more tasks are consolidated, MTF maintains a constant capacity for plasticity by ensuring that each task occupies a metrically minimal, but topologically distinct, footprint. By factorizing the representation into a stable topological skeleton and plastic metric warps, MTF reframes the bias-variance tradeoff from a fundamental limitation of learning to a manageable problem of manifold orchestration. Forgetting is characterized not as an inevitable consequence of parameter updates, but as a symptom of *metric overlap*, a condition that MTF explicitly prevents through factorization.

### 6.3 Implications for ML systems.

**Intelligence as geometric control.** The central implication of our analysis is that intelligence should be understood as a form of *geometric control* Jurdjevic (1997), not as improved search Russell and Norvig (1995). On semantically complex state spaces, Theorem 7 shows that no single smooth metric landscape can support globally funnel-shaped descent. Consequently, failures commonly attributed to insufficient capacity or optimization instead reflect a mismatch between topology and metric structure. MTF reframes intelligence as the ability to identify the correct topological context and deploy an appropriate metric geometry within it, thereby transforming intractable global optimization problems into locally contractive inference.

**MTF as a geometric resolution of stability-plasticity.** MTF resolves the stability-plasticity dilemma Mermilliod et al. (2013) by making the tradeoff *structural* rather than *parametric*: what must remain stable is not a particular set of weights, but the *topological scaffold* that encodes reachability and basin structure, while what may remain plastic is the *metric controller* that fits local costs and curvatures on top of that scaffold. In cognitive science McClelland et al. (1995), MTF is the geometric realization of *Structure-before-Specificity* in spatial cognition Tolman (1948): an agent first learns a robust quotient-like map of the task space (a navigation graph of equivalence classes under perceptual aliasing), and only then refines task-specific precision through metric adaptation. Symmetrically, MTF implements *Search-before-Stabilization* in temporal control Sutton et al. (1999): exploration and routing occur primarily in the topological channel (selecting homotopy classes/discrete routes that are resilient to noise), after which stabilization is achieved by metric contraction within the chosen basin (fast local control and calibration). By decoupling these roles, MTF prevents catastrophic forgetting as metric parameters change French (1999): metric updates deform trajectories *within* fixed topological regions rather than tearing or re-gluing the regions themselves, so long-term structure persists while short-term control remains flexible Buzsáki (1996).

**Topology as the locus of abstraction.** MTF suggests that abstraction resides primarily in topology rather than geometry Edelsbrunner and Harer (2010). Topological variables encode task identity, equivalence classes, and global constraints, while metric structure governs efficiency and precision. This view contrasts with representation learning paradigms that seek increasingly expressive embeddings to absorb all variation Bengio et al. (2013). Instead of expanding representational capacity indefinitely, MTF compresses experience by reusing metric structure across topologically aligned tasks. Abstraction, in this sense, is the act of identifying which variations matter and which can be absorbed geometrically Brouwer (1913). For artificial systems, MTF suggests a design principle that differs fundamentally from scaling-based approaches Shen et al. (2024). Rather than increasing model size to absorb task variation, systems should explicitly represent and manipulate topological structure. This has implications for continual learning Wang et al. (2024), meta-learning Hospedales et al. (2021), reinforcement learning Sutton et al. (1998), and foundation models Bommasani (2021), where failures under distributional or structural shift may reflect unmodeled topological change rather than insufficient training. In such settings, improvements may come from better topological indexing rather than more aggressive optimization.

**Limitations and open questions.** Our analysis is formulated for smooth manifolds and relies on Morse-theoretic structure, which raises several open issues for realistic learning systems. First, many environments are naturally discrete or only approximately manifold-structured (e.g., graphs, hybrid systems, or partially observed state spaces), where the appropriate analogs of critical points, indices, and handle attachments require discrete Morse theory or related combinatorial formalisms Edelsbrunner and Harer (2010). Second, the topological condensation step must be implemented from finite samples. In practice, spectral signatures are estimated from approximate neighborhood graphs and are therefore sensitive to sampling density, noise, and graph-construction hyperparameters Chung (1997). Characterizing when signatures are stable enough for reliable switching, and when uncertainty in  $\Sigma$  should trigger cautious exploration rather than commitment, is an important direction. Third, memory indexing and subspace allocation introduce design tradeoffs Miller et al. (2016): larger banks and richer routing improve expressivity Graves et al. (2016), but increase computation and raise the risk of fragmentation (over-partitioning experience into too many signatures). Finally, while our theory motivates a clean separation between topological identification and metric contraction, practical instantiations will require approximations to both components (e.g., learned or quantized keys, approximate eigensolvers, and finite-rank projectors). A systematic understanding of the tradeoffs between expressivity, noise robustness, and computational cost remains open.

**Conclusion.** MTF reframes intelligence as the ability to resolve geometric incompleteness through *representational factorization*. On semantically complex spaces, globally funnel-shaped descent cannot be achieved by a single smooth landscape; robust behavior therefore requires identifying the correct topological context and deploying a compatible metric geometry within it. By separating topological switching (task identity) from memory-amortized metric inference (efficient contraction), MTF provides a principled route to stability and plasticity without resorting to weight freezing or exhaustive search. From this perspective, intelligence is not defined by the depth of computation spent navigating a labyrinth, but by the ability to control the geometry in which inference unfolds.

## Acknowledgments and Disclosure of Funding

This work was partially supported by NSF IIS-2401748 and BCS-2401398. The author has utilized Gemini 3.0 Pro and ChatGPT 5.2 models to aid in the development of theoretical ideas, the design of Colab experiments, and the generation of visual illustrations presented in this paper.

## Appendix A. Proof of Lemma and Theorems

### Proof [Proof of Lemma 6]

We use standard Morse theory; see Milnor (1963).

**Part (1): Vanishing of intermediate homology.** Let  $\beta_i(\mathcal{M}) = \text{rank } H_i(\mathcal{M}; \mathbb{R})$ . For a Morse function  $E$  on a compact manifold, the *weak Morse inequalities* state that

$$c_i(E) \geq \beta_i(\mathcal{M}) \quad \text{for } i = 0, 1, \dots, d. \quad (6)$$

By assumption,  $c_k(E) = 0$  for each  $1 \leq k \leq d - 1$ . Substituting into (6) yields

$$0 = c_k(E) \geq \beta_k(\mathcal{M}) \Rightarrow \beta_k(\mathcal{M}) = 0 \quad \text{for all } 1 \leq k \leq d - 1.$$

Over the field  $\mathbb{R}$  this implies  $H_k(\mathcal{M}; \mathbb{R}) = 0$  for all intermediate degrees, proving (1).

**Part (2): Contractibility under a single minimum.** Assume now that  $E$  has exactly one critical point and it is a minimum:  $c_0(E) = 1$  and  $c_i(E) = 0$  for all  $i \geq 1$ . Under the transversality hypothesis on  $\nabla E$  at the boundary, Morse theory provides a handle decomposition of  $\mathcal{M}$  obtained by attaching an  $i$ -handle for each critical point of index  $i$  (Milnor, 1963, Ch. 3). Since there are no critical points of index  $i \geq 1$ , the decomposition attaches only a single 0-handle and no higher handles. A 0-handle is diffeomorphic to a  $d$ -disk  $D^d$ . Therefore  $\mathcal{M}$  is diffeomorphic to  $D^d$ , and in particular is contractible.

Equivalently, one may argue via sublevel sets: for  $a$  below the unique critical value, the sublevel set  $\mathcal{M}^a = \{x : E(x) \leq a\}$  is empty, and after passing the unique index-0 critical value it becomes a 0-handle  $D^d$ . With no further critical points, no further handle attachments occur, so  $\mathcal{M} = \mathcal{M}^b \cong D^d$  for any  $b$  above the critical value. Hence  $\mathcal{M}$  is contractible.

■

### Proof [Proof of Theorem 7]

We use standard Morse theory; see Milnor (1963).

**Step 1: Morse inequalities force intermediate indices.** Let  $E : \mathcal{M} \rightarrow \mathbb{R}$  be a Morse function. Denote by  $c_i(E)$  the number of critical points of Morse index  $i$ . Let  $\beta_i(\mathcal{M}) = \text{rank } H_i(\mathcal{M}; \mathbb{R})$  be the Betti numbers. The *weak Morse inequalities* state that

$$c_i(E) \geq \beta_i(\mathcal{M}) \quad \text{for all } i = 0, 1, \dots, d. \quad (7)$$

(Over a field such as  $\mathbb{R}$ , these follow from the Morse chain complex and the fact that its homology is isomorphic to singular homology.)

By semantic complexity, there exists some  $k \in \{1, \dots, d-1\}$  with  $\beta_k(\mathcal{M}) > 0$ . Applying (7) at index  $k$  yields

$$c_k(E) \geq \beta_k(\mathcal{M}) > 0,$$

so  $E$  has at least one critical point of index  $k$ , where  $1 \leq k \leq d-1$ . This proves (1).

**Step 2: Intermediate index implies saddle under gradient flow.** Fix a Riemannian metric  $g$  on  $\mathcal{M}$  and consider the gradient flow  $\dot{z} = -\nabla_g E(z)$ . Let  $p$  be a nondegenerate critical point of  $E$  with Morse index  $k$ . In  $g$ -normal coordinates at  $p$ , the Hessian  $\text{Hess}_p(E)$  is symmetric and nonsingular. The linearization of the flow at  $p$  is

$$\dot{\xi} = -(\text{Hess}_p(E))\xi.$$

Since the Morse index of  $p$  is  $k$ , the Hessian has exactly  $k$  negative eigenvalues and  $d-k$  positive eigenvalues. Therefore  $-\text{Hess}_p(E)$  has  $k$  positive eigenvalues and  $d-k$  negative eigenvalues, so the equilibrium  $p$  has both expanding and contracting directions whenever  $1 \leq k \leq d-1$ . Hence  $p$  is a saddle-type (hyperbolic) equilibrium. This completes the dynamical interpretation in (1).

**Step 3: No-saddle obstruction.** Suppose for contradiction that there exists a Morse function  $E$  on  $\mathcal{M}$  whose critical points have only indices 0 and  $d$ . Then for every  $i \in \{1, \dots, d-1\}$  we have  $c_i(E) = 0$ . Applying the weak Morse inequalities (7) yields

$$0 = c_i(E) \geq \beta_i(\mathcal{M}) \Rightarrow \beta_i(\mathcal{M}) = 0 \quad \text{for all } 1 \leq i \leq d-1,$$

contradicting semantic complexity. Thus no such Morse function exists, proving (2). (Equivalently: any structurally stable Lyapunov landscape in the Morse class must contain an intermediate-index critical point.)

**Step 4: Genericity.** A classical theorem of Thom implies that Morse functions are residual (in particular dense) in  $C^r(\mathcal{M})$  for  $r \geq 2$ ; see (Milnor, 1963, Ch. 3). Therefore, given any  $C^2$  function  $E$  and  $\varepsilon > 0$ , there exists a Morse function  $\tilde{E}$  with  $\|E - \tilde{E}\|_{C^2} < \varepsilon$ . By Step 1 applied to  $\tilde{E}$ ,  $\tilde{E}$  must have an intermediate-index critical point. This proves (3). ■

### Proof [Proof of Theorem 14]

Fix  $x \in \text{supp}(\mathcal{T}_A)$  and write  $z = \Phi_\theta(x)$ . After updating  $\theta \mapsto \theta + \Delta\theta_B$ , we have  $z' = z + \Delta z$  with  $P_A \Delta z = 0$ . The updated condensed representation is

$$\hat{z}'_A(x) = P_A \tilde{W}_A(z + \Delta z) = P_A \tilde{W}_A z + P_A \tilde{W}_A \Delta z.$$

Using the subspace-supported warp property (4),

$$P_A \tilde{W}_A \Delta z = P_A \tilde{W}_A P_A \Delta z = P_A \tilde{W}_A \cdot 0 = 0.$$

Hence  $\hat{z}'_A(x) = \hat{z}_A(x)$  for all  $x$  in the support of task  $A$ . If  $\mathcal{L}_A$  depends on  $\theta$  only through  $\hat{z}_A$  and a task-specific readout, then  $\delta \hat{z}_A = 0$  implies the first-order variation of  $\mathcal{L}_A$  vanishes, i.e.,  $\mathcal{L}_A(\theta + \Delta\theta_B) = \mathcal{L}_A(\theta) + o(\|\Delta\theta_B\|)$ . ■

## References

P.-A. Absil, Robert Mahony, and Rodolphe Sepulchre. *Optimization Algorithms on Matrix Manifolds*. Princeton University Press, Princeton, NJ, 2008. ISBN 978-0-691-13298-3.

Zeyuan Allen-Zhu, Yuanzhi Li, and Zhao Song. A convergence theory for deep learning via over-parameterization. In *International conference on machine learning*, pages 242–252. PMLR, 2019.

Shun-Ichi Amari. Natural gradient works efficiently in learning. *Neural computation*, 10(2):251–276, 1998. Foundational work on coupling the metric tensor to the information geometry of the data.

Roberto Battiti. First-and second-order methods for learning: between steepest descent and newton’s method. *Neural computation*, 4(2):141–166, 1992.

Mikhail Belkin and Partha Niyogi. Laplacian eigenmaps for dimensionality reduction and data representation. *Neural Computation*, 15(6):1373–1396, 2003. doi: 10.1162/089976603321780317.

Yoshua Bengio, Aaron Courville, and Pascal Vincent. Representation learning: A review and new perspectives. *IEEE transactions on pattern analysis and machine intelligence*, 35(8):1798–1828, 2013.

Rishi Bommasani. On the opportunities and risks of foundation models. *arXiv preprint arXiv:2108.07258*, 2021.

Léon Bottou, Frank E Curtis, and Jorge Nocedal. Optimization methods for large-scale machine learning. *SIAM Review*, 60(2):223–311, 2018.

Luitzen Egbertus Jan Brouwer. Intuitionism and formalism. *Bulletin of the American Mathematical Society*, 20:81–96, 1913. URL <https://plato.stanford.edu/entries/brouwer/>. English translation (A. Dresden) of Brouwer’s 1912 inaugural lecture *Intuitionisme en Formalisme*.

György Buzsáki. The hippocampo-neocortical dialogue. *Cerebral cortex*, 6(2):81–92, 1996.

Fan RK Chung. *Spectral graph theory*, volume 92. American Mathematical Soc., 1997.

Herbert Edelsbrunner and John Harer. *Computational Topology: An Introduction*. American Mathematical Society, Providence, RI, 2010. ISBN 9780821849255.

Babak Esmaeili, Robin Walters, Heiko Zimermann, and Jan-Willem van de Meent. Topological obstructions and how to avoid them. *Advances in Neural Information Processing Systems*, 36:8865–8884, 2023.

Mehrdad Farajtabar, Navid Azizan, Alex Mott, and Ang Li. Orthogonal gradient descent for continual learning. In *Proceedings of the 23rd International Conference on Artificial Intelligence and Statistics (AISTATS)*, volume 108 of *Proceedings of Machine Learning Research*, pages 3762–3773, 2020. URL <https://proceedings.mlr.press/v108/farajtabar20a.html>.

Mark I. Freidlin and Alexander D. Wentzell. *Random Perturbations of Dynamical Systems*. Grundlehren der mathematischen Wissenschaften. Springer, Berlin, Heidelberg, 2012. ISBN 9781468401769. doi: 10.1007/978-3-642-25847-3.

Robert M French. Catastrophic forgetting in connectionist networks. *Trends in cognitive sciences*, 3(4):128–135, 1999.

Stuart Geman, Elie Bienenstock, and René Doursat. Neural networks and the bias/variance dilemma. *Neural computation*, 4(1):1–58, 1992.

Samuel Gershman and Noah Goodman. Amortized inference in probabilistic reasoning. In *Proceedings of the annual meeting of the cognitive science society*, volume 36, 2014.

Kurt Gödel. *On Formally Undecidable Propositions of Principia Mathematica and Related Systems*. Dover Publications, New York, 1962. English translation of the 1931 paper, with introduction by R. B. Braithwaite.

Ian Goodfellow. *Deep learning*. MIT press, 2016.

Andrzej Granas, James Dugundji, et al. *Fixed point theory*, volume 14. Springer, 2003.

Alex Graves, Greg Wayne, Malcolm Reynolds, Tim Harley, Ivo Danihelka, Agnieszka Grabska-Barwińska, Sergio Gómez Colmenarejo, Edward Grefenstette, Tiago Ramalho, John Agapiou, et al. Hybrid computing using a neural network with dynamic external memory. *Nature*, 538(7626):471–476, 2016. doi: 10.1038/nature20101. URL <https://www.nature.com/articles/nature20101>.

Victor Guillemin and Alan Pollack. *Differential Topology*. Prentice-Hall, Englewood Cliffs, NJ, 1974. ISBN 9780132126050.

Allen Hatcher. *Algebraic topology*. Cambridge University Press, 2002.

Nicholas J. Higham. *Functions of Matrices: Theory and Computation*. Society for Industrial and Applied Mathematics, Philadelphia, PA, 2008. ISBN 9780898716467. doi: 10.1137/1.9780898717778.

Morris W. Hirsch. *Differential Topology*, volume 33 of *Graduate Texts in Mathematics*. Springer, New York, NY, 1976. ISBN 9781468494495. doi: 10.1007/978-1-4684-9449-5.

Morris W. Hirsch, Stephen Smale, and Robert L. Devaney. *Differential Equations, Dynamical Systems, and an Introduction to Chaos*. Academic Press, 3 edition, 2012.

Timothy Hospedales, Antreas Antoniou, Paul Micaelli, and Amos Storkey. Meta-learning in neural networks: A survey. *IEEE transactions on pattern analysis and machine intelligence*, 44(9):5149–5169, 2021.

Lei Huang, Yi Zhou, Fan Zhu, Li Liu, and Ling Shao. Iterative normalization: Beyond standardization towards efficient whitening. In *Proceedings of the IEEE/CVF Conference on Computer Vision and Pattern Recognition (CVPR)*, 2019.

Witold Hurewicz and Henry Wallman. *Dimension theory*, volume 4. Princeton university press, 2015.

Velimir Jurdjevic. *Geometric Control Theory*. Cambridge University Press, Cambridge, 1997. ISBN 9780521495028.

Jared Kaplan, Sam McCandlish, Tom Henighan, Tom B. Brown, Benjamin Chess, Rewon Child, Scott Gray, Alec Radford, Jeffrey Wu, and Dario Amodei. Scaling laws for neural language models. *arXiv preprint arXiv:2001.08361*, 2020.

Hassan K. Khalil. *Nonlinear Systems*. Prentice Hall, 3 edition, 2002.

James Kirkpatrick, Razvan Pascanu, Neil Rabinowitz, Joel Veness, Guillaume Desjardins, Andrei A Rusu, Kieran Milan, John Quan, Tiago Ramalho, Agnieszka Grabska-Barwinska, et al. Overcoming catastrophic forgetting in neural networks. *Proceedings of the national academy of sciences*, 114(13):3521–3526, 2017.

John M. Lee. *Introduction to Riemannian Manifolds*, volume 176 of *Graduate Texts in Mathematics*. Springer, 2 edition, 2018.

James Martens. New insights and perspectives on the natural gradient method. *Journal of Machine Learning Research*, 21(146):1–76, 2020.

Nicolas Y. Masse, Gregory D. Grant, and David J. Freedman. Alleviating catastrophic forgetting using context-dependent gating and synaptic stabilization. *Proceedings of the National Academy of Sciences*, 115(44):E10467–E10475, 2018. doi: 10.1073/pnas.1803839115.

James L McClelland, Bruce L McNaughton, and Randall C O'Reilly. Why there are complementary learning systems in the hippocampus and neocortex: insights from the successes and failures of connectionist models of learning and memory. *Psychological review*, 102(3):419, 1995.

Michael McCloskey and Neal J Cohen. Catastrophic interference in connectionist networks: The sequential learning problem. In *Psychology of learning and motivation*, volume 24, pages 109–165. Elsevier, 1989.

Martial Mermilliod, Aurélia Bugaiska, and Patrick Bonin. The stability-plasticity dilemma: investigating the continuum from catastrophic forgetting to age-limited learning effects. *Frontiers in Psychology*, 4:504, 2013. doi: 10.3389/fpsyg.2013.00504. URL <https://PMC.ncbi.nlm.nih.gov/articles/PMC3732997/>.

Alexander Miller, Adam Fisch, Jesse Dodge, Amir-Hossein Karimi, Antoine Bordes, and Jason Weston. Key-value memory networks for directly reading documents. In *Proceedings of the 2016 Conference on Empirical Methods in Natural Language Processing (EMNLP)*, pages 1400–1409, 2016. doi: 10.18653/v1/D16-1147.

John Milnor. *Morse Theory*, volume 51 of *Annals of Mathematics Studies*. Princeton University Press, 1963.

Vardan Papyan, X. Y. Han, and David L. Donoho. Prevalence of neural collapse during the terminal phase of deep learning training. *Proceedings of the National Academy of Sciences*, 117(40):24652–24663, 2020. doi: 10.1073/pnas.2015509117.

German I. Parisi, Ronald Kemker, Jose L. Part, Christopher Kanan, and Stefan Wermter. Continual lifelong learning with neural networks: A review. *Neural Networks*, 113:54–71, 2019. doi: 10.1016/j.neunet.2019.01.012.

Sebastian Ruder. An overview of gradient descent optimization algorithms. *arXiv preprint arXiv:1609.04747*, 2016.

Stuart Russell and Peter Norvig. *Artificial Intelligence: A Modern Approach*. Prentice-Hall, Englewood Cliffs, 1995.

Gobinda Saha, Isha Garg, and Kaushik Roy. Gradient projection memory for continual learning. *arXiv preprint arXiv:2103.09762*, 2021. URL <https://arxiv.org/abs/2103.09762>.

Noam Shazeer, Azalia Mirhoseini, Krzysztof Maziarz, Andy Davis, Quoc V. Le, Geoffrey E. Hinton, and Jeff Dean. Outrageously large neural networks: The sparsely-gated mixture-of-experts layer. *arXiv preprint arXiv:1701.06538*, 2017.

Li Shen, Yan Sun, Zhiyuan Yu, Liang Ding, Xinmei Tian, and Dacheng Tao. On efficient training of large-scale deep learning models. *ACM Computing Surveys*, 57(3):1–36, 2024.

Norman Steenrod. *The Topology of Fibre Bundles*. Princeton University Press, Princeton, NJ, 1951. ISBN 9780691080550.

Richard S Sutton, Andrew G Barto, et al. *Reinforcement learning: An introduction*, volume 1. MIT press Cambridge, 1998.

Richard S. Sutton, Doina Precup, and Satinder Singh. Between MDPs and semi-MDPs: A framework for temporal abstraction in reinforcement learning. *Artificial Intelligence*, 112(1–2):181–211, 1999. doi: 10.1016/S0004-3702(99)00052-1.

Edward C. Tolman. Cognitive maps in rats and men. *Psychological Review*, 55(4):189–208, 1948. doi: 10.1037/h0061626.

Paul Urysohn. Zum metrizationsproblem. *Mathematische Annalen*, 94(1):309–315, 1925.

Liyuan Wang, Xingxing Zhang, Hang Su, and Jun Zhu. A comprehensive survey of continual learning: Theory, method and application. *IEEE transactions on pattern analysis and machine intelligence*, 46(8):5362–5383, 2024.

Patrick M Wensing and Jean-Jacques Slotine. Beyond convexity—contraction and global convergence of gradient descent. *Plos one*, 15(8):e0236661, 2020.

Stephen Willard. *General topology*. Courier Corporation, 2012.